Heliyon 5 (2019) e02465

Contents lists available at ScienceDirect

Heliyon

journal homepage: www.heliyon.com

Physicochemical properties of alpha-mangostin loaded nanomeulsions prepared by ultrasonication technique

Rathapon Asasutjarit [a,*], Tunradee Meesomboon [a], Pheeraphong Adulheem [a], Siriporn Kittiwisut [b], Papawee Sookdee [c], Worada Samosornsuk [d], Asira Fuongfuchat [e]

[a] Novel Drug Delivery Systems Development Center, Department of Pharmaceutical Sciences, Faculty of Pharmacy, Thammasat University, Pathum Thani, 12120, Thailand
[b] Medical Chemistry and Natural Products Research Unit, Department of Pharmaceutical Sciences, Faculty of Pharmacy, Thammasat University, Pathum Thani, 12120, Thailand
[c] Department of Applied Thai Traditional Medicine, College of Allied Health Sciences, Suan Sunandha Rajabhat University, Samut Songkhram, 75000, Thailand
[d] Department of Medical Technology, Faculty of Allied Health Sciences, Thammasat University, Pathum Thani, 12120, Thailand
[e] National Metal and Materials Technology Center, National Science and Technology Development Agency, Thailand Science Park, Pathum Thani, 12120, Thailand

ARTICLE INFO

Keywords:
Infectious disease
Physical chemistry
Pharmaceutical chemistry
Pharmacology
Materials safety
Ultrasonication
Alpha-mangostin
Acnes vulgaris
Formulation
Skin toxicity
Nanoemulsion
Transdermal drug delivery
Mangoteen pericarps extract
Antibacterial activity
Physicochemical properties
Nanomaterials
Materials application

ABSTRACT

Hypothesis: Alpha-mangostin (AMG) is a natural compound possessing strong antibacterial activity. Because of its poor water solubility, the formulations of AMG usually require high concentrations of solubilizers leading limitation for using in some clinical applications. Thus, the novel formulation of topical nanoemulsion (NE) containing AMG (AMG-NE) with optimal content of the oil phase and surfactants was developed.
Experiments: AMG was extracted, purified and used as an active ingredient of AMG-NE. Blank NEs (NEs without AMG) with varying in contents of the oil phase and surfactants and AMG-NE were prepared by the ultrasonication technique. They were investigated their physicochemical properties including antibacterial activity against *Staphyloccocus aureus* and *Propionibacterium acnes* (which is recently renamed as *Cutibacterium acnes*).
Findings: Blank NEs and AMG-NE had droplet size in a range of nanometer and negative value of zeta potential. The droplet size, polydispersity index and zeta potential of blank NEs were affected by formulation compositions and sonication intensities. AMG could be loaded into a representative Blank NE at a maximum concentration of 0.2% w/w and did not cause significant changes in physicochemical properties. AMG-NE showed the antibacterial activity against *Staphyloccocus aureus* and *Propionibacterium acnes* without toxicity to the skin cells. Therefore, AMG-NE had potential for using in a clinical study to investigate its efficacy and safety in patients.

1. Introduction

Alpha-mangostin (AMG) is a major xanthone in fruit pericarps, bark and dried sap of the mangosteen tree (*Garcinia mangostana* Linn.). It was one of xanthones that first isolated in A.D. 1855 from the pericarps of the mangosteen fruit [1]. AMG has various pharmacological activities, including antioxidant, anticancer and anti-inflammatory activities [2, 3, 4, 5]. More importantly, AMG exhibits strong antimicrobial activity against various pathogens, such as methicillin-resistant *Staphylococcus aureus* [6], vancomycin-resistant *Enterococci* [7], and acne-inducing *Propionibacterium acnes* (*P. acnes*) [8, 9], which is recently renamed as *Cutibacterium acnes* (*C. acnes*) [10, 11]. Consequently, AMG has recently been used either as a substitution or as an adjuvant for antibiotics in the treatment of some infectious diseases, especially acnes vulgaris, to decrease problems arising from antibiotic overuse [12, 13].

Because of the hydrophobic characteristics of AMG, its bioavailability is quite limited [14]. The health products that contain AMG usually require a high content of alcohol and surfactants for solubilization of AMG [12, 15]. Sometimes, the solid dispersions of AMG in suitable polymers would also be prepared for circumventing this problem [14]. To avoid toxicities from high concentrations of such solubilizers and complicated techniques in the production process, this study focused on the development of oil in water nanoemulsion (NE) formulations to generate an AMG-loaded nanoemulsion (AMG-NE) containing optimized

* Corresponding author.
E-mail addresses: rathapona@hotmail.com, rathapon@tu.ac.th (R. Asasutjarit).

https://doi.org/10.1016/j.heliyon.2019.e02465
Received 1 May 2019; Received in revised form 10 August 2019; Accepted 9 September 2019
2405-8440/© 2019 European Society for Vascular Surgery. Published by Elsevier B.V. All rights reserved.

content of the oil phase and surfactants.

Presently, health products containing either AMG or mangosteen pericarp extract for topical applications, such as acne gels, cleansing lotions, wound antiseptics, are widely available in the market. Nevertheless, the products containing AMG in a form of NE for the treatment of common skin infections by *Staphylococcus aureus* (*S. aureus*) and *P. acnes,* have not been available. Consequently, the novel formulation of AMG-NE was developed in this study. The investigation not only for its physicochemical properties, but also for its activity against *S. aureus* and *P. acnes*.

Nanoemulsions (NEs) are a type of emulsions that consist of very fine droplets of the internal phase, around 50–500 nm in diameter, dispersed in the external phase. The superior advantages of NEs, as compared to macroemulsions, are high stability against sedimentation, low viscosity and high solubilization capacity, as well as a pleasant aesthetic character and skin feel [16]. Droplet sizes of NEs sometimes are in the same range of microemulsions (less than 100 nm); however, NEs are not thermodynamically stable. For this reason, they cannot form spontaneously, but need energy for droplet formation via either a high-energy or a low-energy emulsification technique [17]. The high-energy emulsification technique, i.e. high shear stirring, high-pressure homogenization and ultrasonication, can provide effective mechanical energy to create droplets and break them into much smaller droplets. This technique can then be used for both laboratory-scale and industrial-scale production of NEs depending on the capacity of instruments [18, 19]. Unfortunately, the low-energy emulsification technique is limited by oil types, emulsifiers and formulation compositions, which affect the spontaneous formation of oil droplets [16]. For this reason, the production of NEs for this study was performed by the high-energy emulsification technique.

The ultrasonication technique is one of the high-energy emulsification methods for NE production. It uses high-frequency sound waves to produce fine droplets of NEs via the ultrasonic homogenizers, which consist of a piezoelectric probe, and generates an intense disruptive force at their tips. When the tip is dipped to the pre-emulsion system, it produces cavitation bubbles. Once the bubbles grow and implode, a jet stream of surrounding liquid and pressurizing dispersed droplets are set up leading to droplet size reduction and high temperature [18]. Since sonication times and input powers are crucial parameters affecting the droplet size and the size distribution of NEs, these parameters need to be optimized for NEs production [16, 20].

The objectives of this study were to determine the effect of formulation compositions and sonication intensities on physicochemical properties of AMG-NE and to investigate antibacterial activity against *S. aureus* and *P. acnes* of the AMG-NE.

2. Materials and methods

2.1. Extraction of AMG from mangosteen fruit pericarps and purification

The dried pericarps mangosteen fruits were ground (Retsch, Germany) and macerated in dichloromethane for 3 days. The crude extract was separated from the marc and then concentrated by using a vacuum rotary evaporator (Büchi, Switzerland). Thereafter, it was purified by the column chromatography (CC) technique [12]. The eluted fractions at every 50 ml containing AMG were collected. AMG powder was obtained after the solvent was removed by using the vacuum rotary evaporator.

2.2. Characterization of AMG

AMG in each 50 ml-eluted fraction from the CC was identified by the thin-layer chromatography (TLC) technique under UV light (at a wavelength of 254 nm) [12]. The R_f values of the components were compared to that of an standard AMG (Chengdu Biopurify Phytochemicals, China). Chemical structure of the obtained AMG was elucidated and confirmed by the Attenuated Total Reflectance-Fourier Transform Infrared (ATR-FTIR) [14], ^{1}H-, ^{13}C Nuclear Magnetic Resonance (NMR) and Mass Spectrometry (MS) technique [21].

The standard AMG powder and the obtained AMG powder were separately characterized by an FT-IR Spectometer (PerkinElmer model Spectrum One, USA). The spectra of all samples were recorded in the wavenumber range of 4,000 to 700 cm^{-1}.

^{1}H and ^{13}C NMR spectra of the obtained AMG were recorded on Ascend TM600 Bruker spectrometer (Switzerland) with the solvent signals as internal standards i.e. 7.19 ppm of residual $CHCl_3$ for ^{1}H and 77.0 ppm of $CDCl_3$ for ^{13}C. Its mass spectra were obtained from an LCMS-IT-TOF, Shimadzu mass spectrometer (Japan). Identification of the obtained AMG was performed by comparison of ^{1}H- NMR, ^{13}C-NMR spectral data and Electrospray Ionization MS (ESI-MS) information to the published data [21].

2.3. Analysis of AMG content

The content of AMG in all samples was analyzed by the high-performance liquid chromatography (HPLC) technique [12]. The analysis was performed by use of an HPLC instrument (Shimadzu UFLC, Japan) equipped with a UV-vis detector for UV detection at 319 nm. A column (Shimadzu, Japan) for separation consisted of a reversed-phase octadecyl column (25 cm × 4.5 mm) with particle size of 5 μm. A mobile phase contained 94% methanol in ultrapure water. It was pumped at a flow rate of 1.0 ml/min at a temperature of 30 °C. Samples were determined in triplicate and calculated for AMG content based on a linear regression equation for a standard curve of AMG.

2.4. Determination of anti-bacterial activity of AMG against S. aureus and P. acnes

The minimum inhibitory concentration (MIC) of AMG *against S. aureus* and *P. acnes* were determined in triplicate by the microdilution assay. *S. aureus* (TISTR No. 1466, Thailand) and *P. acnes* (DMST No. 14914, Thailand) were transferred to Mueller Hilton (MH) broth and Brain-heart infusion (BHI) broth (Merck, Germany), respectively. *S. aureus* was incubated under aerobic conditions for 24 h, whereas *P. acnes* was incubated in anaerobic conditions for 72 h. Thereafter, they were adjusted with normal saline to yield about 10^{6} CFU/ml and dispensed into 96-well plates with a volume of 100 μl for each well. AMG was dissolved in 2% dimethyl sulfoxide (DMSO) (Sigma-Aldrich, USA) to make a concentration of 250 μg/ml as an original concentration before serial two-fold dilutions were made. One hundred μl of each AMG solution was dispensed into wells containing either *S. aureus* or *P. acnes* suspension. These 96-well plates were subsequently incubated under the incubation conditions for either *S. aureus* or *P. acnes*. The MIC of AMG against *S. aureus* and *P. acnes* were the lowest concentration of AMG yielding clear solutions in the wells. In addition, the minimum bactericidal concentration (MBC) of AMG *against S. aureus* and *P. acnes* were further determined by subcultivation of 50 μl of each clear solution in plates containing either MH agar or BHI agar for *S. aureus* or *P. acnes*, respectively. They were incubated under the appropriate incubation conditions. The lowest concentration with no visible growth was defined as the MBC.

2.5. Determination of solubility of AMG

The solubility of AMG in polysorbate 80 (P80), sorbitan oleate (S80), propylene glycol (PG), and an oil phase of the NEs that consisted of mixed oil (a mixture of light mineral oil, cyclomethicone, dimethicone, jojoba oil and capryric/capric triglyceride at a ratio of 1:1:1:1:2, respectively), was determined. One ml of each solvent was added into one gram of AMG contained in a centrifuge tube. The mixture was continuously shaken for 24 h at room temperature and centrifuged at 40,000 rpm for 30 min. The supernatant was filtered through a nylon filter (0.45 μm) and was then analyzed for the AMG content by the HPLC technique.

2.6. Preparation of blank NEs and AMG-NE

The compositions of Blank NEs (NEs without AMG) and AMG-NE prepared in this study were divided into 2 phases, an oil phase and a water phase. The oil phase of NEs contained mixed oil with and without the addition of AMG for the cases of AMG-NE and Blank NEs, respectively. The water phase contained PG, paraben concentrate, mixed surfactant containing P80 and S80 at a ratio of 7:3, respectively, and deionized water.

Blank NEs and AMG-NE were prepared by using the ultrasonication technique. Briefly, the oil phase was blended with mixed surfactant and PG before addition of paraben concentrate and deionized water, respectively. They were stirred by a high-speed homogenizer (Ultra-Turrax T8, Germany) at a rate of 10,000 rpm for 1 min to obtain pre-emulsions. These pre-emulsions were then emulsified by using an ultrasonic homogenizer (Biologics 150VT, USA) with a sonication intensity of 20% amplitude for 5 min. In addition, to investigate the effect of sonication intensity on the physical properties of Blank NEs, the sonication intensity was varied to 10%, 20% and 30% amplitude at a constant sonication time of 5 min.

Droplet size, polydispersity index (PI) and zeta potential of Blank NEs and AMG-NE were evaluated after they were prepared. All Blank NEs and AMG-NE were centrifuged at 5,000 rpm for 30 min and observed for phase separation [22]. The summary of Blank NEs and AMG-NE formulations are shown in Table 1.

Drug entrapment efficiency (EE) and drug loading capacity (LC) of AMG-NE were determined. Briefly, the unentrapped AMG was separated from AMG-NE by using a stirred ultrafiltration cell (Millipore, USA) with an ultrafiltration membrane (MWCO 10 kDa). The filtrate was analyzed for AMG content by the HPLC technique. EE and LC of AMG-NE was calculated by using Eqs. (1) and (2), respectively:

$$\mathrm{EE}(\%) = \frac{\text{total amount of AMG loaded} - \text{amount of unentrapped AMG}}{\text{total amount of AMG loaded}} \times 100 \quad (1)$$

$$\mathrm{LC}\ (\%) = \frac{\text{amount of AMG entrapped in AMG} - \text{NE}}{\text{total amount of lipid and mixed surfactant}} \times 100 \quad (2)$$

2.7. Measurement of droplet size, PI and zeta potential of NEs

Droplet size, that represents the Z-average, and PI of Blank NEs and AMG-NEs were analyzed by the dynamic laser light scattering method using the Zetasizer (Malvern Instrument NanoZS, UK). Their zeta potential was measured by the electrophoretic light scattering technique via the Zetasizer. These properties were measured immediately after preparation in triplicate and reported as a mean ± standard deviation (SD). In particular, the results of droplet size measurement were presented as a mean of the Z-average with SD from particle size distribution histograms.

2.8. Morphology observation of a blank NE and AMG-NE

The morphology of a representative Blank NE and AMG-NE were observed by using transmission electron microscopy (TEM) technique. One drop of diluted samples was placed on a copper grid coated with carbon film, then stained with 1% w/v uranyl acetate solution and allowed to dry under room temperature. The samples were imaged using a JEM-1400 (Japan) transmission electron microscope at an accelerating voltage of 100 kV.

2.9. Rheological properties investigation of a blank NE and AMG-NE

Investigation of rheological properties of a Blank NE and AMG-NE via the steady-shear sweep mode was performed in three replications at 25 ± 0.1 °C. In this study, a controlled stress rheometer (Bohlin Gemini HR nano, Malvern instrument, UK) with a cone and plate geometry (2° cone and 55 mm diameter) was set at 1 and 100 s^{-1} for the initial and final shear rates, respectively.

2.10. Determination of AMG content in AMG-NE

AMG-NE (0.05 g) was dissolved in 94% methanol (5 ml) and then filtered through a 0.45-μm membrane. AMG content in AMG-NE was analyzed by the HPLC technique in three replications following the protocol previously described and reported as a mean ± SD.

2.11. In-vitro release study of AMG-NE

Release of AMG from AMG-NE through a cellulose dialysis membrane was determined by using the modified Franz diffusion cells [23]. In the study, a cellulose dialysis membrane (molecular weight cutoff of 12,000) was placed between the donor unit and the receptor compartment. AMG-NE (2 g) was filled in the donor units and then covered with parafilms. The receiving media used in this study was 10% (v/v) ethanol in PBS (pH = 7.4). It was kept well stirred with a magnetic stirrer and the temperature was maintained at 37 ± 1 °C throughout the study. The receiving media were withdrawn at 5, 10, 20, 30, 60, 120, 180, 240, 300, 360, 420, 480 min and replaced with the same volume of fresh media. AMG content in the receiving media was then determined by the HPLC technique.

Table 1
Summary of formulation compositions of Blank NEs, AMG-NE and their physicochemical properties (mean ± SD; n = 3).

Formulations	Concentrations (%w/w)		AMG (%w/w)	Droplet size[a] (nm)	PI	Zeta potential (mV)	pH	EE	LC	Phase separation[b]
	Mixed oil	Mixed surfactant						(%)	(%)	
5MO-8MS	5	8	0	183 ± 86	0.22 ± 0.03	-2.4 ± 0.3	5.8 ± 0.1	-	-	Not found
10MO-8MS	10	8	0	212 ± 124	0.34 ± 0.02	-5.8 ± 0.2	5.6 ± 0.1	-	-	Not found
15MO-8MS	15	8	0	302 ± 217	0.51 ± 0.10	-7.0 ± 0.2	5.6 ± 0.1	-	-	Not found
10MO-5MS	10	5	0	231 ± 154	0.44 ± 0.04	-6.2 ± 0.3	5.7 ± 0.1	-	-	Not found
10MO-12MS	10	12	0	324 ± 246	0.58 ± 0.04	-4.6 ± 0.2	5.7 ± 0.1	-	-	Not found
10MO-8MS-0.2AMG	10	8	0.2	215 ± 122	0.32 ± 0.02	-6.1 ± 0.2	5.7 ± 0.1	99.24 ± 0.03	1.1 ± 0.00	Not found

[a] Drop size represented the mean of Z-average with SD from particle size distribution histograms.
[b] Phase separation of NEs that was observed after they were centrifuged at 5,000 rpm for 30 min.

2.12. Stability test of AMG-NE

AMG-NE was transferred into tightly sealed glass bottles (25 ml/each) with aluminium foil wrap. The samples were stored at 27 ± 1 °C (an average room temperature in Thailand) for 90 days and observed changes of droplet size, PI, zeta potential, pH, phase separation (without centrifugation) and AMG content at day 0, 30, 60 and 90. For the accelerated stability test, the samples were stored under a heating-cooling condition at 45 ± 1 °C for 48 h and 2 ± 1 °C for 48 h (5 cycles). All samples were evaluated their physicochemical properties in triplicate.

2.13. In-vitro toxicity test of a blank NE and AMG-NE on human skin keratinocytes

Human skin keratinocytes (HaCaT) cells (CLS Cell Line Service, Germany) were cultured in a complete medium, which contained Dulbecco's modified medium (DMEM) and fetal bovine serum (Gibco, USA) (10% v/v). They were seeded in 96-well plates at a density of 1×10^4 cells/well/100 μl and incubated for 24 h in a CO_2 incubator at 37 °C. Thereafter, 100 μl of either a representative Blank NEs or AMG-NE, which were diluted in the complete media at various concentrations, were added to the wells. They were then incubated for 24 h.

After the end incubation period, the cells were washed twice with phosphate buffer saline (PBS) and incubated with 50 μl of methylthiazolydiphenyl tetrazolium bromide (MTT) in DMEM (0.5 mg/ml) for 4 h. The medium was then removed and isopropanol (100 μl/well) was added to each well to dissolve the formazan crystal. The optical density (OD) of each well was determined at 570 nm by a microplate reader (Spectrostar Omega, BMG Labtech, Germany). Percentage of cell viability was calculated using Eq. (3).

$$\text{Cell viability } (\%) = \frac{OD_{sample}}{OD_{control}} \times 100 \quad (3)$$

where OD_{sample} and $OD_{control}$ were the OD of the medium from the wells containing the HaCaT cells incubated with and without the samples, respectively.

The assay of each sample was performed in triplicate and reported as a mean ± SD. The test samples were considered as toxic to the cells if the cell viability was less than 70%.

2.14. Determination of antibacterial activity of AMG-NE against S. aureus and P. acnes

Disc diffusion method was performed to investigate the activity of the AMG-NE against *S. aureus* and *P. acnes*. Briefly, *S. aureus* was transferred to MH broth, and incubated under aerobic condition. Thereafter, it was adjusted with normal saline to yield about 10^8 CFU/ml. The media which contained *S. aureus* were spread thoroughly on the surface of sterile agar, i.e. MH agar. *P. acnes* was prepared in the similar procedures; however, BHI broth and anaerobic incubation were used and sterile agar was BHI with 5% blood agar. Subsequently, the agars that contained bacteria were incubated at 37 °C under aerobic and anaerobic conditions for *S. aureus* (24 h) and *P. acnes* (72 h), respectively. The sterile discs, which had a diameter of 6 mm were impregnated with a representative Blank NE and AMG-NE. They were then carefully laid on the surface of the agars containing bacteria. Following incubation, the diameters of the inhibition zone of each sample were measured. The experiments were performed in three replications. Their antibacterial activities were presented as a mean of inhibition zone diameter (mm) ± SD.

2.15. Statistical analysis

Experimental results were reported as a mean ± SD. Statistical analysis for comparison of treatment effects was performed by either an independent T-test or a one-way ANOVA with Tukey HSD multiple comparisons at a significant level of 0.05.

3. Results and discussion

3.1. Preparation and identification of the obtained AMG

The extraction of dried pericarps of mangosteen fruit yielded 8.18% w/w of a crude extract based on their total weight. This crude extract was further purified by the CC technique, and components in the eluted fraction were identified by the TLC technique. In Fig. 1 (a), the TLC fingerprints of a standard AMG solution (10 μg/ml) and the crude extract of mangosteen fruit pericarps with and without addition of AMG are presented. The TLC fingerprint of the standard AMG solution (Lane A) showed only one band of AMG with an R_f value of 0.50. However, many bands of the components consisting of the crude extract with and without addition of standard AMG appeared in their TLC fingerprints (Lane I and II, respectively). Among these components, one had an R_f value equaling 0.50. In particular, in the case of the TLC fingerprint of crude extract with the addition of AMG, the band of the component possessing the R_f value of 0.50 was darkened. This finding confirmed the presence of AMG in the crude extract before purification.

After purifications by the CC technique, the number of bands, i.e. corresponded to the number of components in each eluted fraction, was markedly decreased (see Fig. 1 (b)). Note that Lane I-IV in Fig. 1 (b) shows the TLC fingerprints of the extract fraction number 5–8, respectively, as representatives. It was found that the major component remaining in these eluted fractions gave an R_f value of 0.50 equaling the R_f value of the standard AMG shown in Lane B of Fig. 1 (b). This finding clearly indicated that AMG was the major compound found in these eluted fractions. Because of the similar TLC fingerprints with fewer bands of impurities in Lane II-IV (Fig. 1. (b)), the corresponding eluted fraction, i.e. fraction number 6–8, were pooled together and then dried by using the evaporator. Finally, the yellowish powder of AMG was obtained and kept in a fridge (2–4 °C) for further study.

3.2. Characterization of the obtained AMG and determination of its purity

The obtained AMG was characterized by the ATR-FTIR technique. Its FT-IR spectrum was compared to that of the standard AMG, as illustrated in Fig. 2 (a)-(I) and (II). It was found that the spectrum of the obtained AMG was similar to that of the standard AMG and consistent with the FT-IR spectra of AMG as reported in the previous publications [12, 24]. Their spectra show characteristic bands of AMG at the wavenumbers of 3, 417–3,248 cm^{-1} and 1,637–1,581 cm^{-1}, which responded to the stretching of hydroxyl (OH) and carbonyl (C=O) group, respectively. The bands at 1,450 cm^{-1} and 1,076 cm^{-1} were also observed. These particular bands indicated the presence of the aromatic C=C and ether (C–O) bonds in the molecular structure of the obtained AMG, respectively, which is illustrated in Fig. 2 (b).

The ^{1}H- NMR, ^{13}C-NMR spectral data including ESI-MS information of the obtained AMG were listed as follows: ^{1}H-NMR (600 MHz, $CDCl_3$): δ13.70 (s, 1H, 1-OH), 6.75 (s, 1H, H-5), 6.33 (br s, 1H, 6-OH), 6.22 (s, 1H, H-4), 5.22 (m, 2H, H-12, H-17), 4.01 (d, $J = 7.2$ Hz, 2H, H-16), 3.73 (s, 3H, 7-O-CH_3), 3.38 (d, $J = 7.3$ Hz, 2H, H-11), 1.77 (s, 3H, H-19), 1.76 (s, 3H, H-15), 1.70 (br s, 3H, H-14), 1.62 (br s, 3H, H-20); ^{13}C-NMR (150 MHz, $CDCl_3$): δ182.0 (C-9), 161.6 (C-3), 160.6 (C-1), 155.8 (C-10a), 155.1 (C-6), 154.6 (C-4a), 142.6 (C-7), 137.0 (C-8), 135.7 (C-18), 132.1 (C-13), 123.2 (C-17), 121.5 (C-12), 112.2 (C-8a), 108.5 (C-2), 103.6 (C-9a), 101.6 (C-5), 93.3 (C-4), 62.0 (7-OCH_3), 26.7 (C-16), 25.9 (C-20), 25.8 (C-14), 21.4 (C-11), 18.3 (C-15), 17.9 (C-19). ESI-MS (m/z): 409.1 $[M\text{-}H]^-$.

These data were in agreement with the results reported in the previous publication [21]. They thus confirmed the molecular structure of the obtained AMG as shown in Fig. 2 (b).

The obtained AMG was further determined for its purity by the HPLC

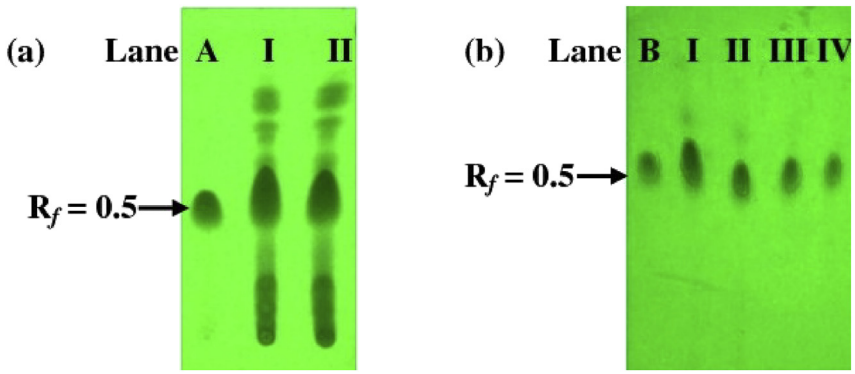

Fig. 1. TLC fingerprints: (a) Lane A: standard AMG, Lane I, II: crude extract of mangosteen fruit pericarps with- and without addition of AMG, respectively; (b) Lane B: standard AMG, Lane I-IV: extract fraction number 5–8, respectively.

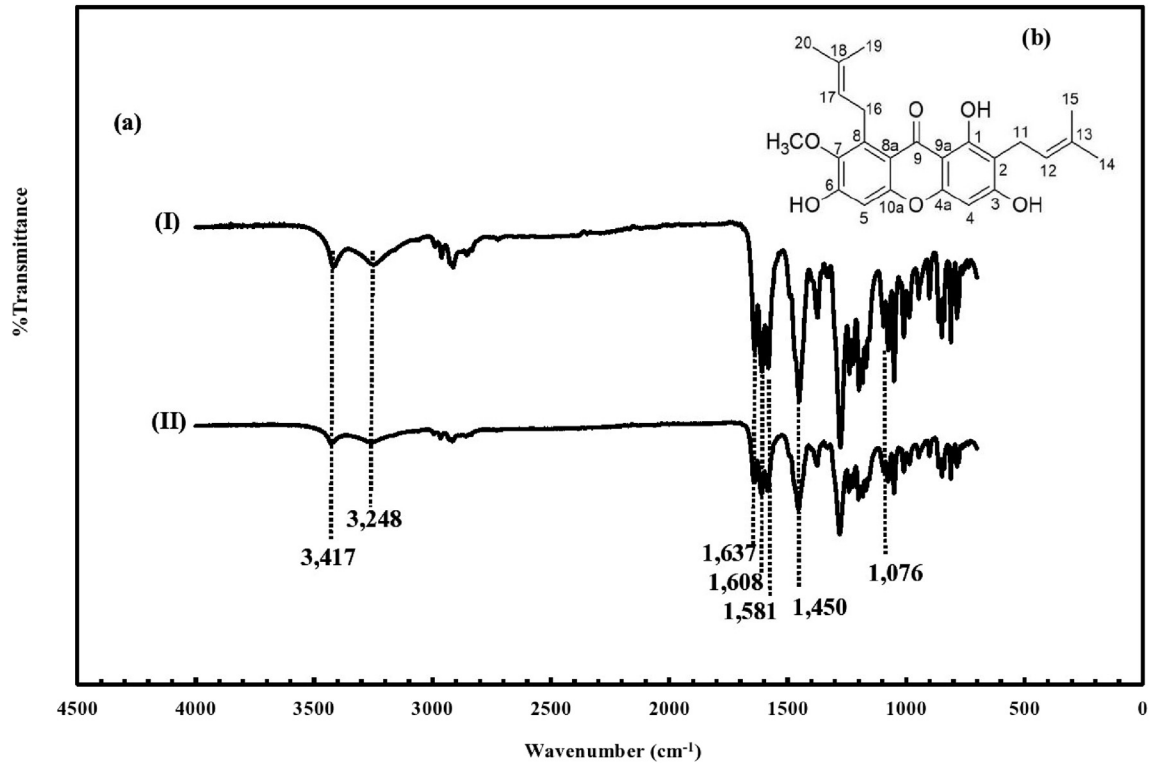

Fig. 2. FT-IR spectra: (a)–(I) standard AMG (II) obtained AMG, and (b) molecular structure of the obtained AMG.

technique. The analysis results showed that the obtained AMG had the same retention time as the standard AMG, at 8.3 min. The AMG content in the extract powder was 80.86% w/w. This result suggested that the AMG obtained from the extraction and purification process in this study had a purity of about 81%. Thus, this particular extract powder could be used for further study and will be referred to as AMG in this article.

3.3. Determination of MIC and MBC of AMG against S. aureus and P. acnes

The results of MIC determination of AMG against *S. aureus and P. acnes* showed that AMG could inhibit the growths of *S. aureus and P. acnes* at the same minimum concentration of 3.9 μg/ml. Meanwhile, AMG could kill these pathogenic bacteria at a minimum concentration of 7.8 μg/ml. These findings suggested that the antibacterial activities of AMG for *S. aureus and P. acnes* increased when their concentrations were increased. The results were consistent with Koh et al. [6], in that AMG had potent anti-gram positive bacteria activities because it could disrupt the cytoplasmic membrane integrity resulting in breakdown and increased permeability of the cell membrane. In addition, its antibacterial activities occurred in a concentration-dependent manner.

3.4. Determination of solubility of AMG

The solubility of AMG in each solvent, i.e. mixed oil, P80, S80 and PG at room temperature, was 15.6 ± 0.0 mg/ml, 1.0 ± 0.0 mg/ml, 0.5 ± 0.0 mg/ml and 1.0 ± 0.0 mg/ml, respectively. It indicated that mixed oil was a good solubilizer for AMG. This property was the result of the hydrophobic characteristics of AMG and the oils in mixed oil [14], and a greater polarity of the other solvents.

3.5. Physicochemical properties of blank NEs and AMG-NE

All Blank NEs prepared in this study exhibited milk-like appearance, i.e. a white color with slight turbidity, and low viscosity. They were, moreover, slightly acidic, i.e. pH ~ 5.6–5.8. Their mean droplet size was

in the range of 183–324 nm with a slightly broad droplet size distribution. The zeta potential values of these NEs were around -2 to -7 mV. All the mentioned properties are presented in Tables 1 and 2. It was found that these properties were affected by formulation compositions and sonication intensity. Furthermore, all Blank NEs showed no phase separation after they were centrifuged at 5,000 rpm for 30 min. The results indicated that these Blank NEs had good physical stability when subjected to gravitational stresses.

3.5.1. Effect of mixed oil content

The droplet size, PI and zeta potential of Blank NEs containing various mixed oil contents are shown in Table 1 (5MO-8MS, 10MO-8MS and 15MO-8MS). It indicated that increments of mixed oil content at a fixed concentration of mixed surfactant (8% w/w) could markedly increase droplet size, PI and zeta potential of Blank NEs (p-value = 0.000, 0.002, 0.000, respectively). This finding could be explained that an increase in mixed oil content led to the higher weight ratios of the internal phase to the external phase and, consequently, the viscosity of the NEs was increased [16, 25]. When NEs were more viscous, the oil droplets were difficult to break during homogenization [25]. Thus, Blank NEs with larger droplet sizes and a broader droplet size distribution were obtained. Table 1 shows that all Blank NEs had low zeta potential because non-ionic emulsifiers were used in the formulations. Nonetheless, the negative zeta potential would result from the negative charge of anionic species consisting of the mixed oil. The results also showed that the negative zeta potential of Blank NEs was increased when the mixed oil content was increased. The previous study reported that the anionic species derived from the free fatty acids in the mixed oil tended to be located near the droplet surfaces and thus affected the surface charge [26, 27]. This may led to the greater negative zeta potential when the mixed oil content was increased in NEs formulation.

Since the formulation of 10MO-8MS provided an NE having optimal values of droplet size, PI and zeta potential, including enough oil content for dissolving AMG, it was used as a prototype for further formulation development.

3.5.2. Effect of surfactant content

The effect of mixed surfactant content in the formulation on droplet size, PI and zeta potential of Blank NEs were evaluated. In this study, the contents of mixed surfactant were adjusted from 5% to 12% w/w at a fixed concentration of mixed oil (10% w/w), and then the obtained NEs were characterized. The results shown in Table 1 pointed out that droplet size, PI and zeta potential of 10MO-5MS, 10MO-8MS, 10MO-12MS were statistically different (p-value = 0.000, 0.000, 0.000). Generally, the droplet size and PI of NEs are inversely proportional to the content of surfactant. This outcome results from the fact that the higher concentration of surfactant was able to provide the sufficient number of the surfactant molecules required to stabilize the internal phase of NEs by reducing interfacial tension and preventing droplet aggregation. It is known that molecules of P80 and S80 are rapidly adsorbed at the droplet interface and provide steric stabilization [18]. Therefore, 10MO-8MS, which contained 8% w/w of mixed surfactant, had smaller droplet size and lower PI than that of 10MO-5MS, which contained 5% w/w of mixed surfactant (p-value = 0.000, 0.018, respectively). However, when the concentration of mixed surfactant was increased to 12% w/w, the droplet size and PI were markedly increased (p-value = 0.000 for both droplet size and PI). This result can be explained that the excess surfactant molecules may accumulate on the droplet surface resulting in droplet destabilization and the larger droplet size. Furthermore, some structures such as mixed micelles and niosomes could be formed leading to variation in size distribution of the system [28].

The zeta potential of Blank NEs was also affected by the content of surfactant. The results in Table 1 indicated that the more surfactant content, the lower zeta potential of the droplets. In this study, 10MO-12MS, which contained the highest content of surfactant, had a lower zeta potential than those of 10MO-8MS and 10MO-5MS, respectively (p-value = 0.000, 0.000, respectively). This result probably resulted from accumulation of non-ionic surfactant molecules at the oil droplet surface shielding the negative charge of anionic species near the droplet surface including the presence of mixed micelles and niosomes [28].

Table 2
Effect of sonication intensity on droplet size, PI and phase separation of 10MO-8MS (mean ± SD; n = 3).

Sonication intensity (% amplitude)	Droplet size[(a)] (nm)	PI	Phase separation[(b)]
10	279 ± 203	0.53 ± 0.01	Not found
20	212 ± 124	0.34 ± 0.02	Not found
30	210 ± 121	0.33 ± 0.01	Not found

[(a)] Drop size represented the mean of Z-average with SD from particle size distribution histograms.
[(b)] Phase separation of NEs that was observed after they were centrifuged at 5,000 rpm for 30 min.

3.5.3. Effect of sonication intensity

10MO-8MS, which had acceptable values of droplet size, PI and zeta potential, and included good stability, was selected for investigation into the effect of sonication intensity in relation to the power of sonication [20] on its droplet size and PI at a constant sonication time of 5 min. The results shown in Table 2 suggested that an increase in sonication intensity from 10% to 20% amplitude could reduce the droplet size and PI of 10MO-8MS properly (p-value = 0.000). Unfortunately, the increment of sonication intensity from 20% to 30% amplitude did not cause further reduction in these parameters. The droplet size and PI of 10MO-8MS, when being exposed to 20% sonication intensity, were comparable to those of 10MO-8MS exposed to 30% sonication intensity at a p-value of 0.368 and 0.844, respectively. The high-amplitude sonication could provide intense shear forces through acoustic cavitation, which generated imploding bubbles and caused micro-jets that impinged upon one liquid, causing it to disperse into the nano-droplets. When sonication intensity was increased, the more efficient droplet disruption occurred, leading to Blank NEs having a smaller droplet size and a lower PI value [29]. However, further increase in sonication intensity would increase the rate of droplet coalescence because surfactant molecules could not be adsorbed on the droplet surface properly, so that the droplet size was not decreased significantly [20]. A similar relationship between droplet size and ultrasonic power was also found in the case of D-limonene NEs using a mixture of sorbitane trioleate and polyoxyethylene (20) oleyl ether as an emulsifier [30]. Consequently, the 20% amplitude was still being used for the preparation of AMG-NEs in subsequent studies.

In this study, the sonication time was fixed constantly at 5 min to avoid overheat that could induce degradation of formulation compositions from long-time exposure to ultrasound waves [19]. Furthermore, this time interval was sufficient to prepare the highly stable Blank NEs that did not show phase separation after being centrifuged, as shown in Table 2.

3.5.4. Effect of AMG

Since MIC and MBC against *S. aureus* and *P. acnes* of AMG were 3.9 μg/ml and 7.8 μg/ml, respectively, the AMG content that was selected for loading into the formulation should provide the concentration that will achieve the antibacterial activity and should be more than these critical concentrations. Because AMG is a low-polarity compound [31], its solubility in water is very low, about 0.2 μg/ml [14]. Therefore, purified water could not be used as a vehicle of AMG for this purpose. Although the solubility of AMG in mixed oil was around 15.6 mg/ml, AMG should be loaded into 10MO-8MS at a concentration of about 0.156 %w/w. However, 10MO-8MS also contained the ingredients that could dissolve AMG, i.e. mixed surfactant and PG. Consequently, AMG could be added

into this formulation up to a concentration of 0.2%w/w with EE around 99% and LC of 1.1% as shown in Table 1.

10MO-8MS-0.2AMG was prepared based on the formulation of 10MO-8MS with the addition of AMG (0.2% w/w). It was emulsified by the ultrasonication method at a sonication intensity of 20% amplitude for 5 min. The obtained product had a pale yellow color, slight turbidity, low viscosity and an acidic pH. Droplet size, PI, zeta potential and pH of 10MO-8MS-0.2AMG as shown in Table 1 were not statistically different from those of 10MO-8MS at a *p*-values of 0.438, 0.789, 0.801 and 0.817 respectively. This result suggested that AMG at 0.2% w/w did not affect the physicochemical properties of 10MO-8MS.

TEM micrographs of 10MO-8MS and 10MO-8MS-0.2AMG are shown in Fig. 3 (a) and (b), respectively. They demonstrate that the oil droplets of 10MO-8MS and 10MO-8MS-0.2AMG were in a nanometer range with slightly broad droplet size distribution, which agreed with the results of droplet size measurement by the dynamic laser light scattering technique. These TEM micrographs illustrate the identically spherical shape and droplet size of oil droplets consisting of the NEs. They confirmed that AMG did not significantly affect the droplet size and PI of the system.

3.6. Rheological properties of a blank NE and AMG-NEs

10MO-8MS and 10MO-8MS-0.2AMG were investigated for their rheological properties. The viscosity profile presented in Fig. 4 (a) indicated that both 10MO-8MS and 10MO-8MS-0.2AMG possessed constant viscosities at entire shear rates, of around 0.002 Pas. Their flow curves, illustrated in Fig. 4 (b), show the linear relationship between shear rate and shear stress, which are represented by the following equations.

$$\text{Shear stress}_{\,10MO\text{-}8MS} = 0.002 \text{ x Shear rate}_{\,10MO\text{-}8MS};\ r^2 = 0.9999 \quad (4)$$

$$\text{Shear stress}_{\,10MO\text{-}8MS\text{-}0.2AMG} = 0.002 \text{ x Shear rate}_{\,10MO\text{-}8MS\text{-}0.2AMG};\ r^2 = 0.9999 \quad (5)$$

These equations indicated that the relationship between shear rate and shear stress of 10MO-8MS and 10MO-8MS-0.2AMG was consistent with Newton's Law of fluid flow. Thus, 10MO-8MS and 10MO-8MS-0.2AMG exhibited a Newtonian flow behavior [32]. The coefficients of Eqs. (4) and (5) implied that 10MO-8MS and 10MO-8MS-0.2AMG had a same viscosity of 0.002 Pas. Therefore, addition of AMG at concentration of 0.2 %w/w also did not affect the flow behavior and the viscosity of 10MO-8MS.

It is important to note that the viscosity of 10MO-8MS and 10MO-8MS-0.2AMG were very low, because they were dilute nanoemulsions with a small volume fraction of the oil phase to the water phase, around 0.1 [33]. The interactions between oil droplets might be from van der Waals forces, which were attractive forces leading to coalescence. However, both NEs still had good stability without phase separation after being centrifuged (Table 1), although they had a low value of zeta potential. Consequently, steric effects from the bulkiness head group of surfactant molecules that were located at the droplet surfaces may protect the droplets from aggregation and coalescence. When shearing forces were applied, the droplets were free to move separately without strong frictions and interactions between droplet surfaces, leading to low flow resistance and flow behaviors of the Newtonian fluid [32, 33]. These findings indicated that 10MO-8MS and 10MO-8MS-0.2AMG could be applied easily on the skin. However, to modify their flow behavior and viscosity, the appropriate polymers could be selected and added into the formulation [19].

3.7. In-vitro release study of AMG-NE

Prior to perform *in-vitro* release study, the content of AMG in AMG-NE was analyzed to investigate the uniformity of the samples that were prepared in this study. Results of analysis showed that the AMG content in 10MO-8MS-0.2AMG was 0.20 ± 0.00 g/100g (n = 3). This value was within a range of 90–110 % of the labeled amount. It revealed that AMG was homogeneously mixed and dispersed in the products. This concentration value was thus used as an initial concentration of AMG in 10MO-8MS-0.2AMG for the release study.

The release profile of 10MO-8MS-0.2AMG illustrated in Fig. 5 (a) shows a fast release of AMG during the first 30 min of the experiment. This finding might have been the result of some AMG that had already been released from the oil droplets into the external phase. Since 10MO-8MS-0.2AMG had low viscosity, the AMG in the external phase was able to diffuse into the receiving media easily [34]. Thereafter, the AMG consisting in the oil droplets was released continuously into the receiving media following a zero-order kinetic model ($r^2 = 1.00$) at a constant rate of 0.12 μg/min, as seen in Fig. 5 (b). The results suggested that the AMG release rate was mainly controlled by an AMG diffusion rate from the droplets and was independent of the concentration of AMG remaining in the droplets [35]. A steady release rate of the AMG over a period of time resulted in possible benefits of 10MO-8MS-0.2AMG. It could prolong the action of AMG with a minimum number of administrations and the side effects of AMG resulting from a reduction in the frequency of usage [35].

3.8. Stability test of AMG-NE

The results of stability test shown in Table 3 suggested that 10MO-8MS-0.2AMG was stable at a room temperature (27 ± 1 °C) for 90 days. Its physicochemical properties and AMG content in the formulation were not significantly changed (*p*-value = 0.519, 0.615, 0.702, 0.679 and 0.086 for droplet size, PI, zeta potential, pH and AMG content, respectively). Furthermore, obvious alterations of these parameters could not be observed after being subjected to the heating-cooling test (*p*-value =

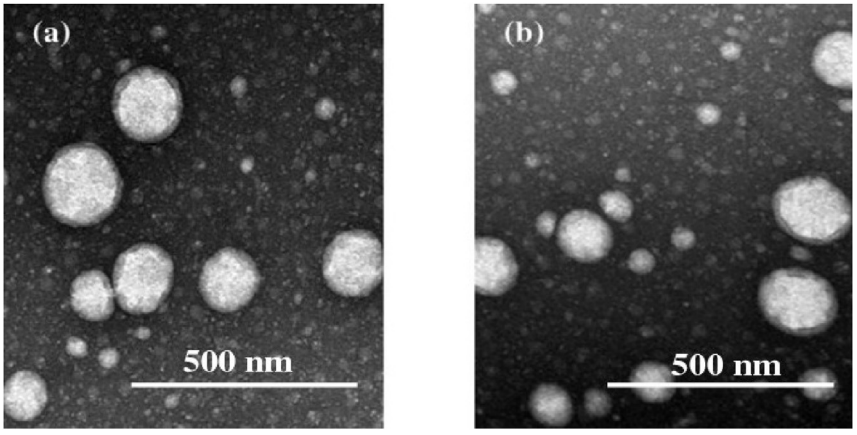

Fig. 3. TEM micrographs: (a) 10MO-8MS and (b) 10MO-8MS-0.2AMG.

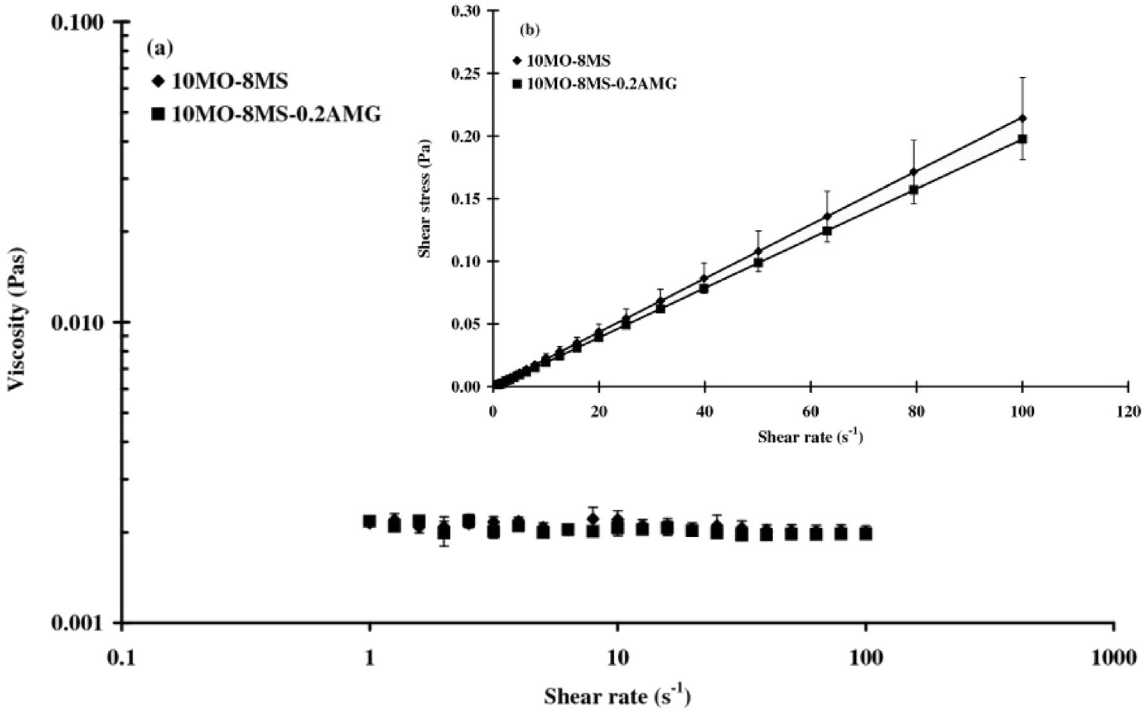

Fig. 4. Rheological properties of 10MO-8MS and 10MO-8MS-0.2AMG: (a) viscosity profiles; (b) flow curves.

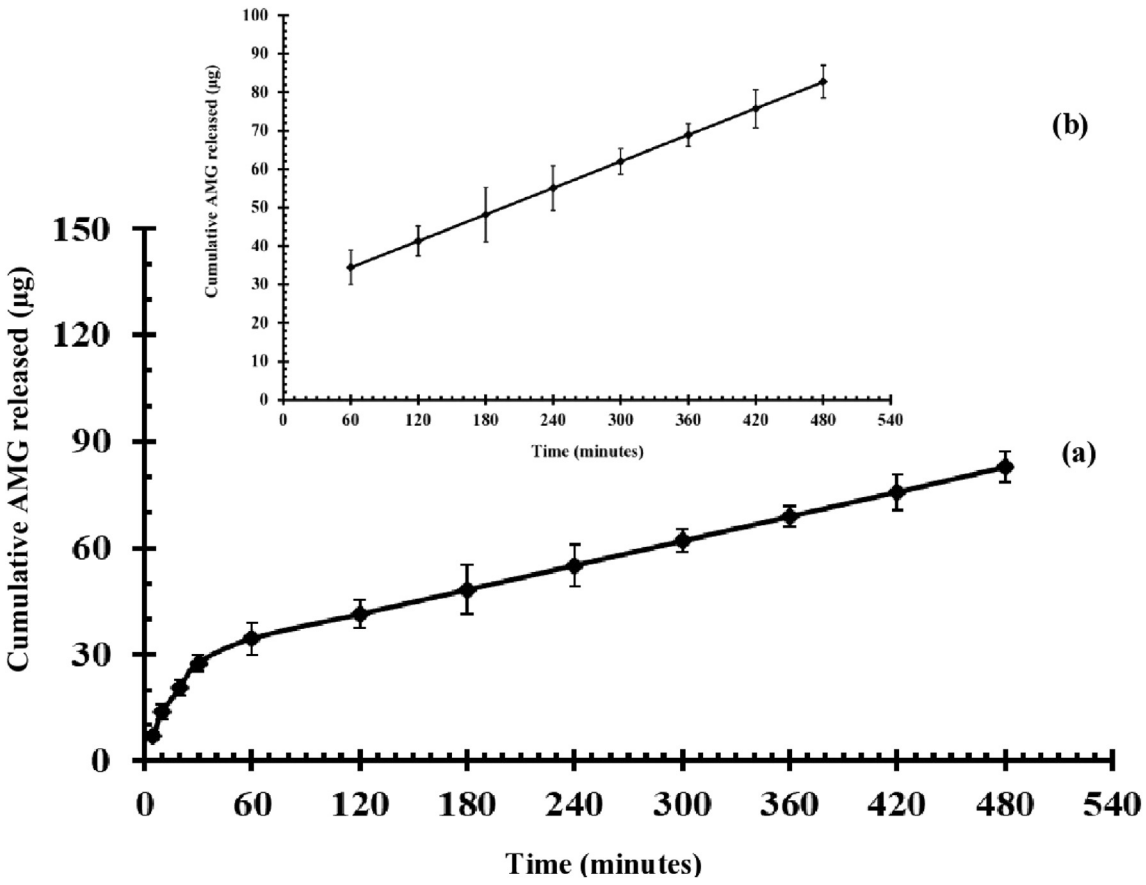

Fig. 5. Release profile of AMG from 10MO-8MS-0.2AMG (mean ± SD, n = 3): (a) cumulative drug released content against time during 0–480 min; (b) cumulative drug released content against time during 60–480 min.

Table 3
Physicochemical properties and AMG content of 10MO-8MS-0.2AMG after storage at a room temperature (27 ± 1 °C) for 90 days and under a heating-cooling test (5 cycles) (mean ± SD; n = 3).

Storage conditions	Droplet size[(a)] (nm)	PI	Zeta potential (mV)	pH	Phase separation[(b)]	AMG content (%w/w)
1) Room temperature						
Day 0	215 ± 122	0.32 ± 0.02	-6.1 ± 0.2	5.7 ± 0.1	Not found	0.20 ± 0.00
Day 30	209 ± 121	0.34 ± 0.03	-6.3 ± 0.2	5.5 ± 0.2	Not found	0.20 ± 0.01
Day 60	212 ± 124	0.30 ± 0.02	-5.9 ± 0.5	5.8 ± 0.4	Not found	0.19 ± 0.01
Day 90	214 ± 126	0.35 ± 0.03	-6.2 ± 0.8	5.5 ± 0.4	Not found	0.19 ± 0.01
2) Heating-cooling test	218 ± 129	0.35 ± 0.04	-5.8 ± 0.5	5.8 ± 0.4	Not found	0.19 ± 0.00

[(a)] Drop size represented the mean of Z-average with SD from particle size distribution histograms.
[(b)] Phase separation of NEs that was observed after they were stored under two different storage conditions without centrifugation.

0.970, 0.766, 0.881, 0.998 and 0.450 for droplet size, PI, zeta potential, pH and AMG content, respectively). This finding would result from the optimized formulation of AMG-NE and production process as previously discussed. Therefore, 10MO-8MS-0.2AMG had acceptable physical and chemical stability and could be used in further studies.

3.9. *In-vitro skin toxicity*

The *in-vitro* skin toxicity tests of 10MO-8MS and 10MO-8MS-0.2AMG on the HaCaT cells were determined by using the MTT assay. Percentage cell viability of the cells at each concentration of the test samples was reported as a mean ± SD, as illustrated in Fig. 6. It was found that the cells could survive in all test samples at entire concentrations within a range of 84–97% cell viability. Although cell viability of HaCaT cells after exposure to 10MO-8MS at each concentration was not significantly different (p-values = 0.101), the obvious difference was found in the case of 10MO-8MS-0.2AMG at a concentration of 5,000 μg/ml (p-values = 0.000). It was lower than that of HaCaT cells exposed to other lower concentrations of 10MO-8MS-0.2AMG. This finding could be explained by the fact that the higher the concentration of 10MO-8MS-0.2AMG, the higher the content of AMG. AMG can generally exhibit cytotoxicity activity towards some human cells, especially cancer cells such as human breast adenocarcinoma and colorectal adenocarcinoma, by inducing apoptosis [1]. AMG at relatively higher concentrations would consequently display some cytotoxicity to normal cells like the normal human bronchus diploid cell line CCD-14Br [36], including the HaCaT cells used in this study.

3.10. *Anti-S. aureus and P. acnes activity of AMG-NE*

10MO-8MS and 10MO-8MS-0.2AMG were investigated for their anti-*S. aureus and P. acnes* activity by using the disc diffusion method. Since the results shown in Table 4 indicated that 10MO-8MS did not generate clear zones in the agar plates containing pathogenic bacteria, 10MO-8MS could not inhibit *S. aureus* and *P. acnes* growth. This finding was probably that the ingredients consisting of 10MO-8MS did not has strong antibacterial activities. Consequently, they could neither inhibit nor kill the bacteria at their current concentration consisting of the formulation. On the other hand, 10MO-8MS-0.2AMG gave clear zones in the plates containing *S. aureus* and *P. acnes*, implying that 10MO-8MS-0.2AMG could inhibit growth of *S. aureus* and *P. acnes*. This outcome was due to the fact that the concentration of AMG released from 10MO-8MS-0.2AMG reached the MIC and MBC against the pathogenic bacteria, 10MO-8MS-0.2AMG could inhibit bacterial growth and kill these bacteria properly. As previously mentioned that AMG had poor aqueous solubility [14], it thus could not diffuse and spread widely in the aqueous-base agar resulting in slightly small diameter of such clear

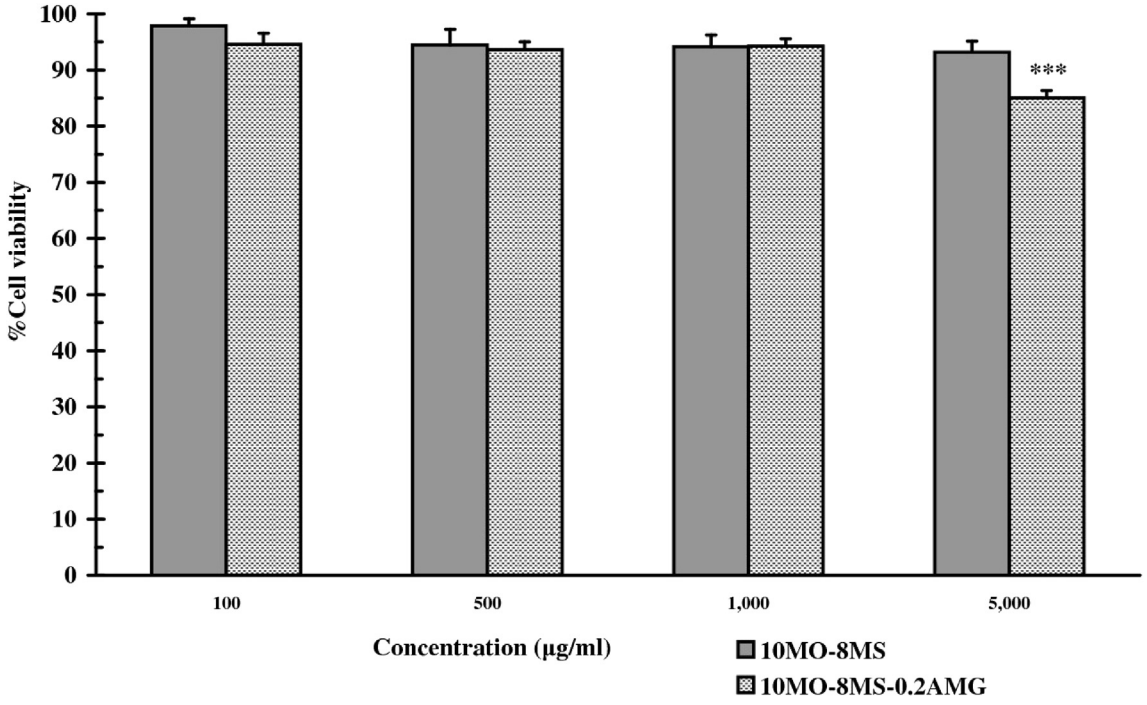

Fig. 6. Cell viability (%) of HaCaT after exposure to 10MO-8MS and 10MO-8MS-0.2AMG at various concentrations (mean ± SD, n = 3) (*significantly different from others at a p-value < 0.05).

Table 4
Diameter of inhibition zones (mean ± SD; n = 3).

Test samples	Diameter of inhibition zones (mm)	
	S. aureus	*P. acnes*
10MO-8MS	0.0 ± 0.0	0.0 ± 0.0
10MO-8MS-0.2AMG	10.0 ± 0.0	7.3 ± 0.6

zones. It was observed that the diameter of clear zones in the agar containing *S. aureus* was larger than that of clear zones in the agar containing *P. acnes* (p-value = 0.016). This result indicated that *S. aureus* was more susceptible to 10MO-8MS-0.2AMG than *P. acnes*. Therefore, 10MO-8MS-0.2AMG could be used for treatment of skin infection caused by *P. acnes* and *S. aureus* in particular.

4. Conclusions

This study showed that the oil in water AMG-NE, which contained the optimized content of oil phase and surfactants, could improve solubility of AMG up to a maximum concentration of 0.2% w/w that was higher than its water solubility of 0.2 μg/ml. Generally, the formulations containing AMG usually require high content of either alcohol or surfactants for dissolving AMG. They sometimes cause skin irritation and limitation for clinical use. Therefore, the development of NE formulation in this study provided a promising delivery system of AMG possessing acceptable physicochemical properties including antibacterial activity for treatment of common bacterial skin infections.

AMG extracted from the mangosteen fruit pericarps and purified in our study had a purity of 81% w/w. AMG could inhibit the growth of *S. aureus* and *P. acnes* and kill these pathogenic bacteria at the same MIC and at the same MBC of 3.9 and 7.8 μg/ml, respectively. After characterization, AMG was used as an active ingredient of the NEs. The results showed that the physicochemical properties of Blank NEs and AMG-NE were affected by formulation compositions and sonication intensity during emulsification by the ultrasonication method. Blank NEs and AMG-NE that were prepared in this study had droplet size in the nanometer range, slightly broad droplet size distribution, negative value of zeta potential and acidic pH value. It was found that an increment in the mixed oil content in Blank NEs formulation led to an increase in droplet size, PI and zeta potential. However, the effect of mixed surfactant content was dependent on its concentration in the formulation. At low concentrations of mixed surfactant, not higher than 8% w/w, an increase in mixed surfactant content resulted in a reduction in droplet size and PI. When the concentration of mixed surfactant was increased to 12% w/w, both droplet size and PI increased. Unfortunately, it was found that the more there was of surfactant content, the lower there was of zeta potential of the droplets. Droplet size and PI of Blank NEs were also affected by sonication intensity. It was found that an increase in sonication intensity to 20% amplitude could reduce droplet size and PI. Nevertheless, an increment of sonication intensity to 30% amplitude did not cause a significant reduction of these parameters. To prepare AMG-NE, AMG was added to the formulation at a concentration of 0.2% w/w. It was found that AMG at this concentration did not affect droplet size, PI or zeta potential, pH, including the rheological properties of NEs. The release kinetic of AMG from AMG-NE was in agreement with the zero-order release kinetic model. AMG-NE exhibited the antibacterial activity against *S. aureus* and *P. acnes* without toxicity to skin cells. Therefore, AMG-NE had potential for use in a clinical study to investigate its efficacy and safety in patients.

Declarations

Author contribution statement

Asira Fuongfuchat: Conceived and designed the experiments; Performed the experiments; Contributed reagents, materials, analysis tools or data; Wrote the paper.

Rathapon Asasutjarit: Conceived and designed the experiments; Performed the experiments; Analyzed and interpreted the data; Contributed reagents, materials, analysis tools or data; Wrote the paper.

Worada Samosornsuk, Papawee Sookdee, Siriporn Kittiwisut, Pheeraphong Adulheem & Tunradee Meesomboon: Performed the experiments; Analyzed and interpreted the data.

Funding statement

The authors gratefully acknowledge the National Research Council of Thailand, Thammasat University and the National Science and Technology Development Agency (NSTDA) for the financial support under The Research Grant No.51/2561 (The fiscal year 2018) and the Young Scientist and Technologist Programme (YSTP) grant No. SCA–CO–2560-4651-TH and No. SCA–CO–2561-7238-TH, academic year 2017 and 2018, respectively.

Competing interest statement

The authors declare no conflict of interest.

Additional information

No additional information is available for this paper.

References

[1] J. Pedraza-Chaverri, N. Cárdenas-Rodríguez, M. Orozco-Ibarra, J.M. Pérez-Rojas, Medicinal properties of mangosteen (*Garcinia mangostana*), Food Chem. Toxicol. 46 (10) (2008) 3227–3239.
[2] M.Y. Ibrahim, N.M. Hashim, A.A. Mariod, S. Mohan, M.A. Abdulla, S.I. Abdelwahab, et al., α-Mangostin from *Garcinia mangostana* Linn: an updated review of its pharmacological properties, Arab. J. Chem. 9 (3) (2016) 317–329.
[3] G.A. Mohamed, A.M. Al-Abd, A.M. El-halawany, H.M. Abdallah, S.R.M. Ibrahim, New xanthones and cytotoxic constituents from *Garcinia mangostana* fruit hulls against human hepatocellular, breast, and colorectal cancer cell lines, J. Ethnopharmacol. 198 (2017) 302–312.
[4] F. Gutierrez-Orozco, C. Chitchumroonchokchai, G.B. Lesinski, S. Suksamrarn, M.L. Failla, α-Mangostin: anti-inflammatory activity and metabolism by human cells, J. Agric. Food Chem. 61 (16) (2013) 3891–3900.
[5] S. Syam, A. Bustamam, R. Abdullah, M.A. Sukari, N.M. Hashim, S. Mohan, et al., β Mangostin suppress LPS-induced inflammatory response in RAW 264.7 macrophages *in vitro* and carrageenan-induced peritonitis in vivo, J. Ethnopharmacol. 153 (2) (2014) 435–445.
[6] J.-J. Koh, S. Qiu, H. Zou, R. Lakshminarayanan, J. Li, X. Zhou, et al., Rapid bactericidal action of alpha-mangostin against MRSA as an outcome of membrane targeting, Biochim. Biophys. Acta 1828 (2) (2013) 834–844.
[7] Y. Sakagami, M. Iinuma, K.G.N.P. Piyasena, H.R.W. Dharmaratne, Antibacterial activity of α-mangostin against vancomycin resistant Enterococci (VRE) and synergism with antibiotics, Phytomedicine 12 (3) (2005) 203–208.
[8] M.T. Chomnawang, S. Surassmo, V.S. Nukoolkarn, W. Gritsanapan, Effect of Garcinia mangostana on inflammation caused by *Propionibacterium acnes*, Fitoterapia 78 (6) (2007) 401–408.
[9] H. Azimi, M. Fallah-Tafti, A.A. Khakshur, M. Abdollahi, A review of phytotherapy of acne vulgaris: perspective of new pharmacological treatments, Fitoterapia 83 (8) (2012) 1306–1317.
[10] B. Dréno, S. Pécastaings, S. Corvec, S. Veraldi, A. Khammari, C. Roques, *Cutibacterium acnes* (*Propionibacterium acnes*) and acne vulgaris: a brief look at the latest updates, J. Eur. Acad. Dermatol. Venereol. 32 (S2) (2018) 5–14.
[11] E. Platsidaki, C. Dessinioti, Recent advances in understanding *Propionibacterium acnes* (*Cutibacterium acnes*) in acne, F1000Res 7 (2018) F1000. Faculty Rev-953.
[12] R. Asasutjarit, P. Larpmahawong, A. Fuongfuchat, V. Sareedenchai, S. Veeranondha, Physicochemical properties and anti-Propionibacterium acnes activity of film-forming solutions containing alpha-mangostin-rich extract, AAPS PharmSciTech 15 (2) (2013) 306–316.
[13] P. Pan-In, A. Wongsomboon, C. Kokpol, N. Chaichanawongsaroj, S. Wanichwecharungruang, Depositing α-mangostin nanoparticles to sebaceous gland area for acne treatment, J. Pharmacol. Sci. 129 (4) (2015) 226–232.
[14] A.F.A. Aisha, Z. Ismail, K.M. Abu-Salah, A.M.S.A. Majid, Solid dispersions of α-mangostin improve its aqueous solubility through self-assembly of nanomicelles, J. Pharm. Sci. 101 (2) (2012) 815–825.
[15] K. Mulia, G.A. Putri, E. Krisanti, Encapsulation of mangosteen extract in virgin coconut oil based nanoemulsions: preparation and characterization for topical formulation, Mater. Sci. Forum 929 (2018) 234–242.
[16] M.N. Yukuyama, D.D.M. Ghisleni, T.J.A. Pinto, N.A. Bou-Chacra, Nanoemulsion: process selection and application in cosmetics – a review, Int. J. Cosmet. Sci. 38 (1) (2016) 13–24.

[17] L.L. Lee, N. Niknafs, R.D. Hancocks, I.T. Norton, Emulsification: mechanistic understanding, Trends Food Sci. Technol. 31 (1) (2013) 72–78.
[18] Y. Singh, J.G. Meher, K. Raval, F.A. Khan, M. Chaurasia, N.K. Jain, et al., Nanoemulsion: concepts, development and applications in drug delivery, J. Control. Release 252 (2017) 28–49.
[19] V.K. Rai, N. Mishra, K.S. Yadav, N.P. Yadav, Nanoemulsion as pharmaceutical carrier for dermal and transdermal drug delivery: formulation development, stability issues, basic considerations and applications, J. Control. Release 270 (2018) 203–225.
[20] A.M. Hashtjin, S. Abbasi, Optimization of ultrasonic emulsification conditions for the production of orange peel essential oil nanoemulsions, J. Food Sci. Technol. 52 (5) (2015) 2679–2689.
[21] V. Anggia, A. Bakhtiar, D. Arbain, The Isolation of xanthones from trunk latex of *Garcinia mangostana* Linn. and their antimicrobial activities, Indones J Chem. 15 (2015) 187–193.
[22] A. Zaid Alkilani, R. Hamed, S. Al-Marabeh, A. Kamal, R. Abu-Huwaij, I. Hamad, Nanoemulsion-based film formulation for transdermal delivery of carvedilol, J. Drug Deliv. Sci. Technol. 46 (2018) 122–128.
[23] R. Asasutjarit, T. Theerachayanan, P. Kewsuwan, S. Veeranodha, A. Fuongfuchat, G.C. Ritthidej, Development and evaluation of diclofenac sodium loaded-N-trimethyl chitosan nanoparticles for ophthalmic use, AAPS PharmSciTech 16 (5) (2015) 1013–1024.
[24] M. Ahmad, B.M. Yamin, A. Mat Lazim, A study on dispersion and characterisation of α-mangostin loaded pH sensitive microgel systems, Chem. Cent. J. 7 (1) (2013) 85.
[25] A. Azeem, M. Rizwan, F.J. Ahmad, Z. Iqbal, R.K. Khar, M. Aqil, et al., Nanoemulsion components screening and selection: a technical note, AAPS PharmSciTech 10 (1) (2009) 69–76.
[26] C. Qian, D.J. McClements, Formation of nanoemulsions stabilized by model food-grade emulsifiers using high-pressure homogenization: factors affecting particle size, Food Hydrocolloids 25 (5) (2011) 1000–1008.
[27] S. Ribes, A. Fuentes, P. Talens, J.M. Barat, G. Ferrari, F. Donsì, Influence of emulsifier type on the antifungal activity of cinnamon leaf, lemon and bergamot oil nanoemulsions against *Aspergillus niger*, Food Control 73 (2017) 784–795.
[28] M.A. Schubert, C.C. Müller-Goymann, Characterisation of surface-modified solid lipid nanoparticles (SLN): influence of lecithin and nonionic emulsifier, Eur. J. Pharm. Biopharm. 61 (1) (2005) 77–86.
[29] A.S. Peshkovsky, S. Bystryak, Continuous-flow production of a pharmaceutical nanoemulsion by high-amplitude ultrasound: process scale-up, Chem. Eng. Process: Process Intensification 82 (2014) 132–136.
[30] P.-H. Li, B.-H. Chiang, Process optimization and stability of d-limonene-in-water nanoemulsions prepared by ultrasonic emulsification using response surface methodology, Ultrason. Sonochem. 19 (1) (2012) 192–197.
[31] M. Guo, X. Wang, X. Lu, H. Wang, P.E. Brodelius, α-Mangostin extraction from the native mangosteen (Garcinia mangostana L.) and the binding mechanisms of α-mangostin to HSA or TRF, PLoS One 11 (9) (2016), e0161566.
[32] P.J. Sinko, A.N. Martin, Martin's Physical Pharmacy and Pharmaceutical Sciences: Physical Chemical and Biopharmaceutical Principles in the Pharmaceutical Sciences, Lippincott Williams & Wilkins, Philadelphia, 2011, pp. 561–563.
[33] M.E. Helgeson, Colloidal behavior of nanoemulsions: interactions, structure, and rheology, Curr. Opin. Colloid Interface Sci. 25 (2016) 39–50.
[34] R. A-sasutjarit, A. Sirivat, P. Vayumhasuwan, Viscoelastic properties of carbopol 940 gels and their Relationships to piroxicam diffusion coefficients in gel bases, Pharm. Res. 22 (2005) 2134–2140.
[35] M. Miastkowska, E. Sikora, J. Ogonowski, M. Zielina, A. Łudzik, The kinetic study of isotretinoin release from nanoemulsion, Colloids Surf., A 510 (2016) 63–68.
[36] T.K.T. Phan, F. Shahbazzadeh, T.T.H. Pham, T. Kihara, Alpha-mangostin inhibits the migration and invasion of A549 lung cancer cells, PeerJ 6 (2018) e5027-e.